

SIMPLE AND FAST DAMAGE IDENTIFICATION ON 6061 ALUMINIUM BASED ON MODE SHAPE CURVATURE

M. A. AMIRUDDIN^{1,*}, N. L. JENAT¹, M. H. C. MAN², M. A. IRFAN¹,
N. A. HAMBALI¹, N. FAWAZI², A. S. NOR HALIM¹

¹Jabatan Teknologi Kejuruteraan Mekanikal, Fakulti Teknologi Kejuruteraan Mekanikal dan Pembuatan, Universiti Teknikal Malaysia Melaka, Ayer Keroh, Melaka, Malaysia

²Mechanical Precision Engineering, Malaysia-Japan International Institute of Technology, Universiti Teknologi Malaysia, 54100 Kuala Lumpur, Malaysia

*Corresponding Author: afiq.amiruddin@utem.edu.my

Abstract

This paper presents a simple and fast approach for the identification of damage to isotropic steel structures. The main contribution of this work is a simplified approach using cubic polynomial regression, unlike previously developed damage identification models that use two specimens. This was achieved by differentiating the mode shape displacement from the mode shape curvature using a central finite difference equation to determine the damaged curve, and subsequently, computing the undamaged curve using a Cubic Polynomial Regression (CPR) model. To validate the accuracy of the model, five specimens with different types of damage (single and double notch) at various depths were simulated. The performance of the model was evaluated against the experimental modal test results. It was found that the presented model was capable of detecting the type of damage (whether single or double notch) in a 6061 Aluminium beam structure. However, when compared to the experimental results, the average difference could reach up to 17% due to external factors. In particular, the performance of the presented model in detecting the location of the damage was inaccurate and imprecise for both the FEA simulation and experimental cases. The CPR model is useful for operators and engineers who require a simple and fast approach to detect damage, but, in terms of accuracy, different techniques must be considered, especially those that are capable of removing and clearing out noise signals.

Keywords: 6061 Aluminium, Cubic polynomial regression, Mode shape curvature, Mode shape displacement, Non-damage identification, Structural damage detection.

1. Introduction

Vibration is a very straightforward occurrence and can be viewed as the swaying of an object about a balance point. An excitation force always causes an object to vibrate. Many methods are used to test vibrations, such as mode, resonance, and excitation methods. Other non-destructive detection method, such as ultrasonic and thermography is relatively high cost of operation and limited to surface types and qualities. Hence, a cost-effective structural health monitoring (SHM) method, vibration-based damage detection methods have received increasing attention for real applications [1]. Aluminium is a strong, lightweight, and inexpensive material [2], but regardless of its strength, it still tends to get damaged. The common types of damage that occur in aluminium are galvanic and pitting corrosion. Galvanic corrosion occurs when aluminium comes into contact with precious metals such as copper and zinc that can cause it to break down, while pitting corrosion occurs when aluminium is placed in a very damp environment in which salts are present. Common dirt and debris can also cause pitting corrosion to occur. The welding process can also create defects in aluminium, where hot cracking is common in aluminium weldments.

Many structural health monitoring (SHM) techniques have been created to detect damage. Vibration-based damage detection has replaced local Non-Destructive Inspection (NDI) as a global NDI. Most of the studies on Vibration Based Damage Detection (VBDD) in mode shape curvature used the Gapped Smoothing Method (GSM) algorithm. Zhong and Yang [3] used the GSM algorithm in their experiment because of its sensitivity in localizing micro damage compared to the natural frequency and damping ratio. A study conducted by Hasrizam and Fawazi [4] showed that the incorporation of the Chebyshev interpolation filter method still produces smear noise within the noise area. In 2009, a study by Yoon et al. [5] concluded that the GSM algorithm using the curvature mode shape creates smear noise, which makes it less accurate in estimating the size of the damage. But in 2015, a study by Rucevskis et al. [6] showed that the GSM algorithm is unable to localize damage accurately owing to the sensitivity of the curve fitting to an outlier.

An examination by Ratcliffe [7] utilized curvature mode shape as a boundary for the discovery of harm in structures. The mode shape information from undamaged and damaged structures are utilized, and it was discovered that curvature mode shape can be a superior marker for damage identification contrasted with the natural frequency. Notwithstanding, this technique requires information from the intact structure, which might be difficult to get in a genuine structure. Abdel Wahab and De Roeck [8] expanded the curvature mode shape strategy by averaging the damage index over all the modes and applying their technique to a concrete bridge. The Gapped Smoothing Method (GSM) presented by Pandey et al. [9] has shown that absolute changes of mode shape curvature are more susceptible to be localized in the region of damage. It has been reported this information could be applied to identify the amount of damage in the structure. The benefit of the GSM contrasted with different strategies is that it does not need information from the whole structure. Notwithstanding, this strategy is not exact for the detection of a big-sized crack because the damage index will create two peaks to indicate the presence of two small-sized cracks instead of one big-sized crack [10].

In this paper, a strategy was proposed to distinguish damage in a structure utilizing the curvature mode shape data from the damaged structure, without requiring information from the undamaged structure. This procedure utilized few estimations information to appraise the undamaged curvature mode shape data, ω_u using the Cubic Polynomial Regression (CPR) strategy. The information was in this way used to ascertain the damage index to decide the area and size of the damage in the structure. This technique is required to empower wide-sized breaks to be distinguished without information from the undamaged structure.

2. Modal Analysis

In this study, the modal analysis was divided into two phases. The first phase was a numerical simulation, where the mode shape displacement was determined based on a finite element (FE) simulation. All the simulation works on the computer were carried out using ABAQUS to identify the mode shape displacements at 51 distinct nodes along the surface of a 6061 Aluminium beam. Then, the data were collected from the FE analysis and differentiated to a second-order Ordinary Differential Equation (ODE) using the centred finite divided difference to obtain the mode shape curvature. The differentiation process was carried out using Microsoft Excel.

To identify the undamaged mode shape curvature without taking into consideration the baseline data, a curve fitting method was implemented. As the Cubic Polynomial Regression (CPR) is the simplest curve fitting method compared to other methods such as the Fourier and Laplace transform methods, the CPR was enforced and applied in this study. The Damage Index (DI) was determined from the CPR, and the results were plotted and compared to the experimental data.

In the second phase, an experimental modal test was performed on five damaged 6061 Aluminium beam specimens, which had different numbers of notches and depths, and one control specimen. In the experiment, an excitation force was applied using a hammer connected to DAQ modules, which led to the propagation of vibrations through the beam. The vibrations could be read as the frequency, and their signal was sent to the accelerometer sensor located at the bottom surface of the beam. Once the accelerometer received the signal, it sent it to the DAQ modules to be converted into a Frequency Response Function (FRF). The ME'Scope software was used to divide the signal in the FRF into three modal parameters, namely, the mode shape, natural frequency, and damping ratio. However, only the mode shape data was considered in this study, and the procedures to determine mode shape curvature, undamaged mode shape curvature, and damage index were the same as mentioned earlier in the first phase.

2.1. Finite element analysis and numerical simulation

In this study, the geometry of the steel beam used by Pandey et al. [9], Hasrizam and Fawazi [4] was applied. To be specific, 6061 Aluminium, with a thickness of 5 mm, 1250 mm in length, and 50 mm in width was used in this experiment. The mode shape data is pulled off from a total of 51 grid points, which are located from 25 mm to 1250 mm. The grids are spaced of 25 mm along the distance. This alloy features medium to high strength. It also has good corrosion resistance, weldability, workability, and machinability.

The test materials consisted of five damaged specimens and one control specimen. Two out of the five damaged specimens had a single notch, while the

other three specimens had double notches. Table 1 and Fig. 1 show the dimensions and diagram of the 6061 Aluminium beam model, respectively, that was used in this study, with a notch to represent the damage.

A Finite Element Analysis (FEA) was carried out using the commercial code, ABAQUS to obtain the vibration responses of the 6061 Aluminium beam model using modal analysis. In the analysis, almost all element types are solid and hexahedral elements.

In this study, three-dimensional continuum solid elements of 20 nodes with reduced integration and second order accuracy (C3D20R) are applied for discretization method on the model, which is the same method used by Hasrizam and Fawazi [4]. The model had the properties of an isotropic material with a young's modulus, density, and Poisson's ratio of 68.9 GPa, 2700 kg/m³, and 0.33, respectively. All the cases had free-free boundary conditions and the first bending mode shape was used for the data processing.

Table 1. Description of the six specimens.

	Zero Notch	Single Notch	Double Notch
Length of Notch (a)	150 mm	150 mm	150 mm
		0.5 mm	0.5 mm
		(S150ND0.5)	(D150ND0.5)
Notch Depth (b)	0.0 mm	1.0 mm	1.0 mm
	(C0ND0)	(S150ND1.0)	(D150ND1.0)
			2.5 mm
			(D150ND2.5)

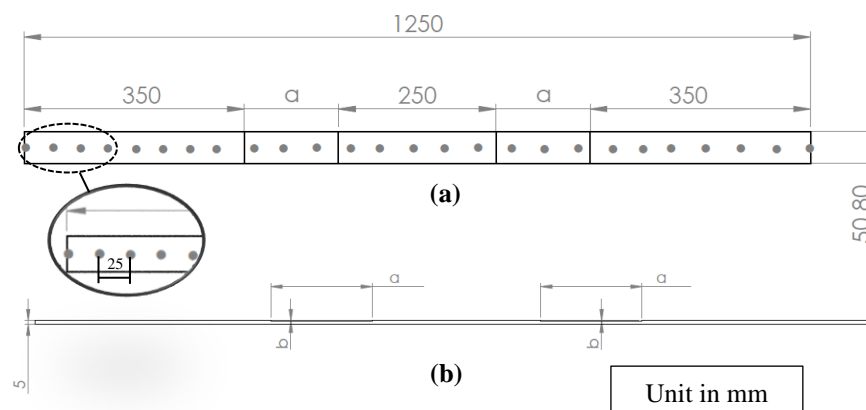


Fig. 1. Diagram of (a) the beam and (b) notch location.

2.2. Experimental modal test

There are many methods for the testing of vibrations. However, in this experiment, a modal test was applied as this method of testing can ascertain the natural frequency (mode), modular mass, modal damping ratio, and mode shape of a sample plate with a perfect impulse. In theory, a perfect impulse, generated by an instrumental hammer, is used to impact the plate, being tested, thereby resulting in a constant amplitude in the frequency domain. Next, the response is measured through the Frequency Response Function (FRF) of an accelerometer, which is placed at one point, known as the driving

point, where the mode shape is adequately excited when the structure is impacted by the hammer. This method, as shown in Fig. 2, is known as the 'roving hammer' test.



Fig. 2. The roving hammer test.

The apparatus was set up as shown in Fig. 3. The accelerometer was placed at the driving point, and only the hammer was moved from node to node. The hammer was used to provide an input force, 5 N, at a specific point on the surface of the beam, and the output from the impact was sent to the accelerometer, which converted the output signal into a voltage. The voltage was then captured by a charge amplifier connected to the front end of the ME'scope, whose function was to convert the signal from analogue to digital form. From there, the ME'scope software displayed the frequency response function, and analysed and interpreted the FRF into a mode shape displacement domain.

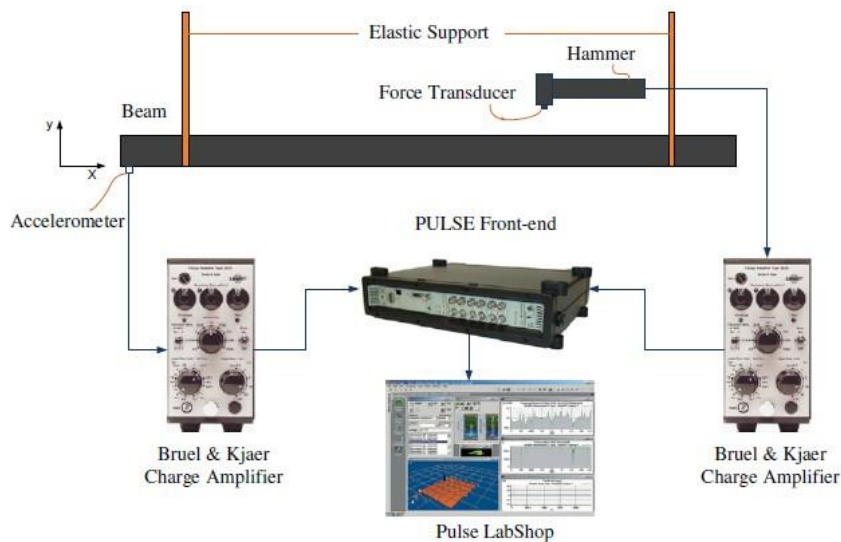


Fig. 3. Diagram of experimental setup.

The 6061 Aluminium beam was knocked with an impact hammer, and the FRF and phase graph were checked on the ME'scope software. If the FRF graph showed the existence of noise, the test at that point had to be redone until the noise was cleared.

2.3. Data analysis procedure

This section presents the data analysis process for this study. Five beams, with different types of damage, were considered in this study. First, the displacement

mode shape data, U_2 from 26 nodes was obtained by performing an FEA, as explained in the earlier section.

Secondly, the curvature mode shape data, ω_u was estimated using the displacement mode shape data, U_2 in the central finite difference equation [9]:

$$\text{Curvature Mode Shape, } \omega_i = \frac{u_{i-1} + 2u_i + u_{i+1}}{\Delta x^2} \quad (1)$$

where u_i is the mode shape at the grid point, i , and Δx is the distance between two successive grid points.

Thirdly, the interpolated curvature mode shape data was fitted using the cubic polynomial regression adapted from the study by Ratcliffe and Bagaria [7, 10, 11]. By means of this process, the fitted curvature mode shape was used as the undamaged curvature mode shape data. The undamaged curvature mode shape data that had been fitted with the cubic polynomial regression was called $\omega_{u|CPR}$. Subsequently, the modal curvature difference or damage index was obtained by subtracting the undamaged curvature mode shape, ω_u from the damaged curvature mode shape, ω_d (calculated using the displacement mode shape data, U_2 from 51 nodes obtained from the FEA that was performed, as explained in an earlier section) given by:

$$\text{Damage Index, } \delta_i^m = |\omega_{d|i} - \omega_{u|i}| \quad (2)$$

where $\omega_{d|i}$ and $\omega_{u|i}$ are the curvature mode shape data at the grid point, i of the damaged and undamaged structures, respectively.

3. Results and Discussion

This section analyses the results of the study from the numerical simulation and experimental tests. The main objective of this study was to detect the size of the crack and identify the damage index in an isotropic material. The simulation data were analysed for 51 nodes, but for the purpose of comparison with the experimental data, only 26 nodes were considered in the analysis to cut down on the time. There were two types of specimens, namely, undamaged, and damaged beams. One specimen or control specimen was considered as the undamaged beam, while five different damaged specimens were taken.

3.1. Numerical simulation and experimental results

The FEA simulation defined the damage size of the crack depth for a single-notched and double-notched beam that was 150 mm in length. The results of the simulation analysis were generated by ABAQUS, as shown in Figs. 4(a) and (b). The graphs of the simulation data for all the specimens, as shown in these figures, had a smooth shape for the mode shape displacement. Only the fundamental bending mode shapes were considered for the data processing.

The distance between the nodes was 25 mm for all the specimens, and the values of the displacement among the specimens are ranged from -0.00251245 mm to 1 mm. From the graph, it was apparent that the length of the mode shape displacement for the double notch with a depth of 2.5 mm (D150ND2.5) was slightly longer and distorted when compared to the control sample (C0ND0). What stood out in this chart was that the growth of the damage or notch in the beam could cause the mode shape displacement tended to elongate further as the integrity of the structure tends to be deteriorated.

The distance between the nodes was 25 mm for all the specimens, and the values of the displacement among the specimens are ranged from -0.00251245 mm to 1 mm. From the graph, it was apparent that the length of the mode shape displacement for the double notch with a depth of 2.5 mm (D150ND2.5) was slightly longer and distorted when compared to the control sample (C0ND0). What stood out in this chart was that the growth of the damage or notch in the beam could cause the mode shape displacement tended to elongate further as the integrity of the structure tends to be deteriorated.

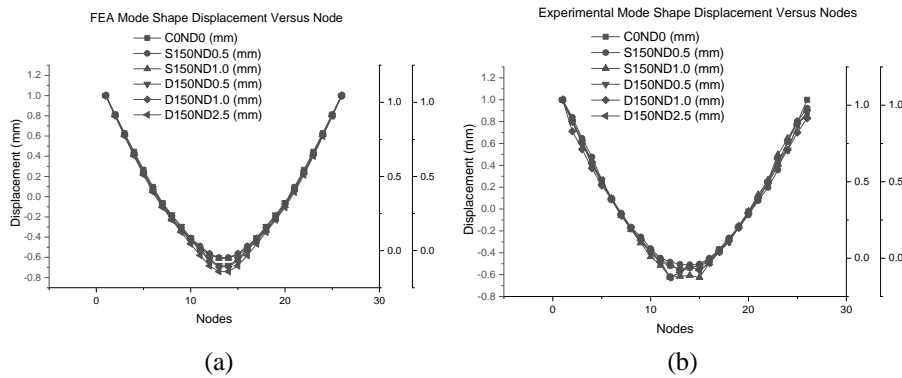


Fig. 4. Graph of mode shape displacement versus node for all specimens (a) FEA simulation (b) Experimental result.

Turning now to the experimental evidence in Fig. 4(b), a comparison of the two results revealed that the experimental result showed an excessiveness in the peak from Node 12 until Node 15. A few factors could have affected the precision or accuracy of the results, such as the elastic support and force when hammering. According to Hanly [12], other environmental factors such as temperature, acoustic noise, humidity, corrosive substances, and shocks and vibrations may affect the results obtained.

Table 2 shows a comparison of the mode shape displacement by the FEA and experimental modal analysis for all the specimens. One interesting finding was that the average of the difference between the experimental and FEA simulation results was less than 17% from nodes 12 until 15 for five specimens, and the overall difference was higher than that of the previously reported difference by Hasrizam and Fawazi [4], which was 3%. This inconsistency may have been due to the possible interference of noise, which cannot be ruled out, during the experimental modal test.

Unfortunately, these findings were rather difficult to interpret, specifically for the experiment, because the differentiation of the second-order ODE to obtain the damaged and undamaged mode shape curvatures led to inaccurate and complex interpretations of the damage index as noise was included in the findings.

3.1.1. Mode shape curvature and damage index

The mode shape curvature method is based on the difference in mode shapes between damaged and undamaged structures, whereas the vector location of the

damage is based on the variability of the damaged and undamaged structures. In this study, the central, forward, and backward finite differences were applied to differentiate the mode shape displacement data into the mode shape curvature.

Table 2. Representation of mode shape displacement data from FEA and experimentation.

Node	Displacement (mm)		Difference (%)
	FEA	Experiment	
Single Notch-0.5 mm depth (S150-0.5)			
12	-0.5628	-0.4848	16.09
13	-0.6026	-0.5057	19.16
14	-0.6026	-0.5092	18.34
15	-0.5628	-0.5023	12.04
Single Notch-1.0 mm depth (S150-1.0)			
12	-0.5685	-0.6248	9.01
13	-0.6084	-0.6151	1.09
14	-0.6084	-0.6078	0.10
15	-0.5685	-0.6259	9.17
Double Notch-0.5 mm depth (D150-0.5)			
12	-0.6222	-0.6245	0.37
13	-0.6785	-0.5808	16.82
14	-0.6785	-0.5265	28.87
15	-0.6222	-0.5617	10.77
Double Notch-1.0 mm depth (D150-1.0)			
12	-0.6363	-0.5144	23.70
13	-0.6929	-0.5484	26.35
14	-0.6929	-0.5312	30.44
15	-0.6362	-0.5174	22.96
Double Notch-2.5 mm depth (D150-2.5)			
12	-0.6838	-0.6244	9.51
13	-0.7399	-0.5808	27.39
14	-0.7399	-0.5265	40.53
15	-0.6838	-0.5617	21.74
Average of Difference (%)			17.22

Figure 5 shows the plot of the curvature mode shape from the FEA simulation data. It was noted that the curvature mode shape for the undamaged beam had a shape that was clean of any irregularity, as shown in Fig. 5(a), while the damaged beam with a single notch had a very small irregularity that was not clearly visible, and the damaged beam with double notches had a big irregularity that was clearly observable. Thus, differences in the curvature mode shape between the damaged and undamaged structures can show the location of the damage in the structures. The single most striking observation to emerge from the comparison of the data between the FEA and experimentally controlled specimens was the noise signals that emerged in the chart.

The damage index plot is an indicator of the presence of damage in a structure. It is calculated by subtracting the undamaged curvature mode shape, $\omega_{u|i}$ from the damaged curvature mode shape, $\omega_{d|i}$. In addition, the size, and location of a crack in the structure can be estimated from the damage index plot. Figure 6 shows the damage index for the single and double-notch cases. It should be noted that the CPR is able to detect the location of the damage, but it is not highly accurate compared to other methods such as Chebyshev filters (CFs) and the Gap Smoothing Method (GSM) [4].

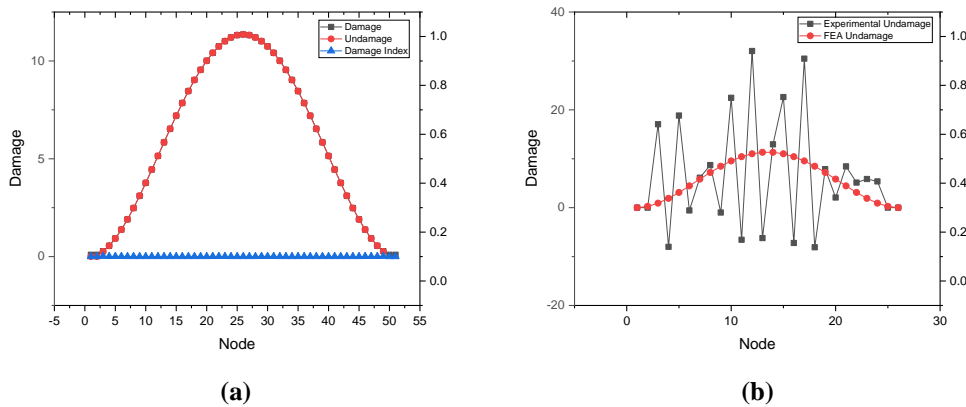
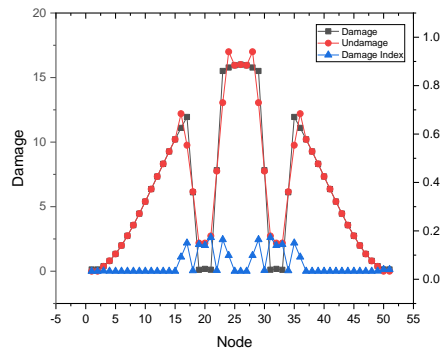


Fig. 5. Controlled specimen without a notch (COND0) (a) Comparison within FEA Simulation and (b) Comparison FEA and experimental undamaged.

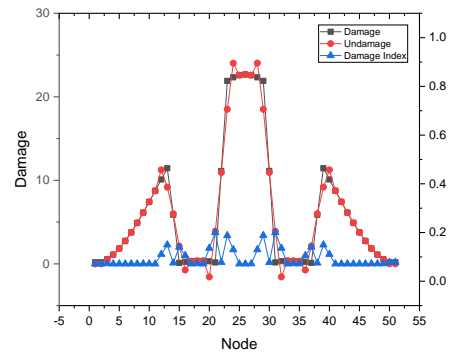
In Figs. 6(a) and 6(b), the CPR indicated the presence of the damage index of two nearby small notches between Node 15 and Node 25, and Node 27 and Node 37, which were false detections. In Figs. 6(c), 6(d), and 6(e), the cubic polynomial regression indicated the presence of the damage index of four small notches between Node 10 to Node 17, Node 20 to Node 25, Node 27 to Node 33, and Node 35 to Node 43, which were also false detections.

Some authors have speculated that the lack of filter capability causes the cubic polynomial regression to produce a deviation in the curvature mode shape data rather than in the damaged curvature mode shape, and the difference is indicated in the damage index as a false damage detection [4]. However, despite its inaccuracy and imprecision, the CPR method was still able to identify the damage for both the single and double-notch specimens. According to the chart in Figs. 6(c), 6(d), and 6(e), the double-notch chart had multiple spikes in the damage index compared to the charts of the single-notch and control specimens in Figs. 6(a) and 6(b). Besides, the chart pattern among double-notch specimens are no significant differences.

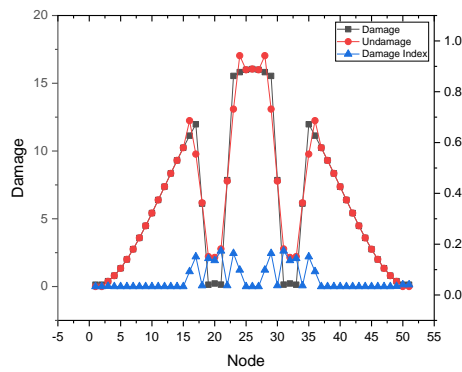
To verify the simulation results, an experimental modal test was carried out, and the standard damage index was implied. Figure 7 shows that the standard damage index of COND0 from the experiment was larger than the simulation result for the same specimen. This test showed that several points at Node 4, Node 6, and Node 12 implied high peaks. COND0 supposedly should not have had any damage or spike as there was no damage or notch along the beam.



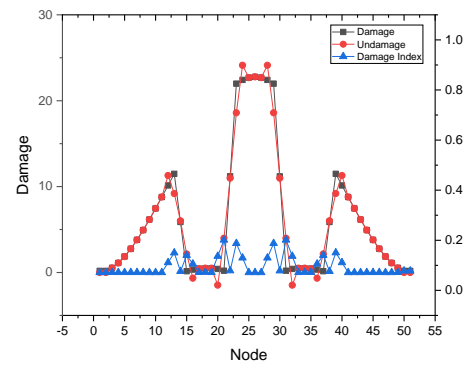
(a)



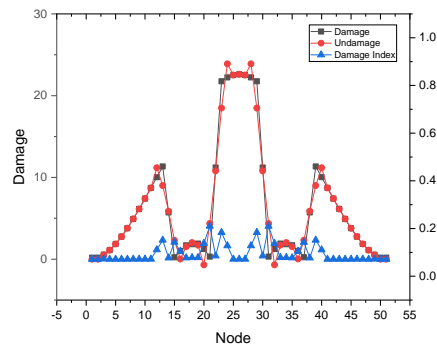
(c)



(b)



(d)



(e)

Fig. 6. FEA simulation of curvature mode shape plot for
(a) Single notch 0.5 mm depth (S150ND0.5) (b) Single notch 1.0 mm depth (S150ND1.0)
(c) Double notch 0.5 mm depth (D150ND0.5) (d) Double notch 1.0 mm depth (D150ND1.0)
(e) Double notch 2.5 mm depth (D150ND2.5).

Figures 8(a)-8(e) show that damage was presented on the structures or beams, which had single and double notches with depths of 0.5 mm and 1.0 mm, respectively. However, the findings of this experiment did not support the FEA results. There are several possible explanations for these findings. These results could possibly have been due to the lack of an adequate filter for the CPR, which caused a deviation in the mode shape curvature between the damaged and undamaged structures, and the difference was implied as a false damage detection [4].

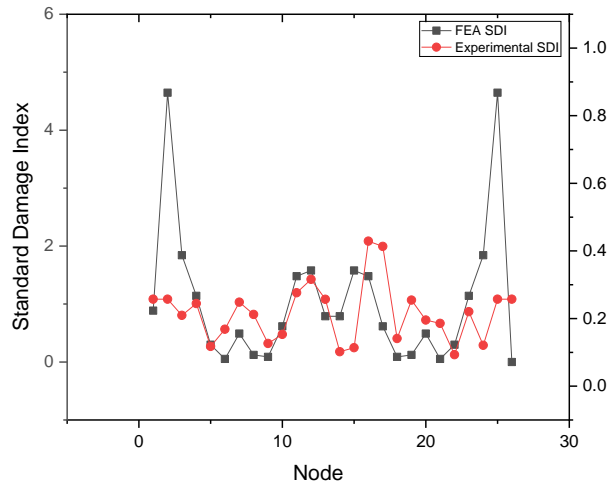


Fig. 7. Standard damage index of FEA and experimental test for the controlled specimen (COND0).

Another possible explanation for this is that during the analysis, it was observed that certain factors affected the precision of the outcome. One factor was the versatile help and power when pounding. The elastic band that was utilized as the versatile help would, in general, become stretchy after a few uses or after a period of time. This could have affected the base outcome or the results of each experiment. The excessive amount of power that was exerted when pounding could likewise have influenced the precision of the data that was gathered or obtained. At some point, when the amount of power put into the pounding was frail, the pounding effect might not have been delivered properly through the drive point that was joined to the accelerometer.

Other ecological factors, for example, temperature, acoustic commotion, stickiness, destructive substances, and shocks and vibrations, may have influenced the outcome. As indicated by Hanly [12], each of the above elements can fundamentally influence the exactness of the information acquired at the time when the data is taken or when the trial is carried out.

In this investigation, a piezoelectric accelerometer was utilized as a sensor. In accordance with the present results, Hanly [12] has explained that this sensor may have had some reliance on the temperature. To counterbalance this impact, the requirement for temperature is fundamental. He also expounds the accelerometer could likewise have been influenced by acoustic clamour or weight waves that could have energized the accelerometer and the sample during the trial. Likewise, Hanly [12] elucidates that the humidity could have influenced the exactness of the data, as it can cause issues at the link associations and cause the hardware to be

questionable, particularly with old gears, where the seals might be broken or worn out. At the point when the hardware was presented to muggy conditions, it would, in general, consume and this would prompt the gathering of wrong information or data. To wrap things up, shocks and vibrations might be factors that cause deviations in the base outcome or information, and the use of an electronic sensor in the field may not be appropriate for use in the laboratory.

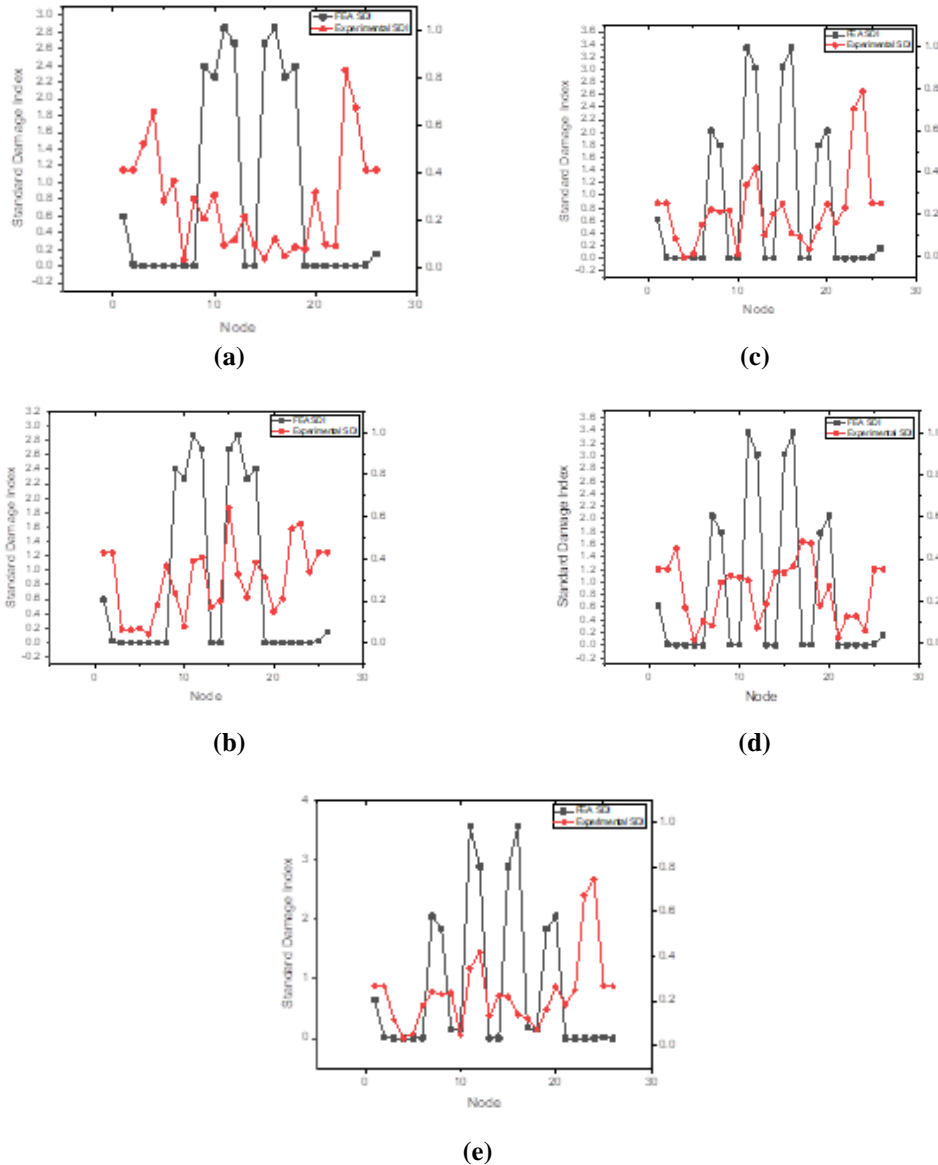


Fig. 8. Standard damage index of FEA and experimental test for (a) Single notch 0.5 mm depth (S150ND0.5), (b) Single notch 1.0 mm depth (S150ND1.0), (c) Double notch 0.5 mm depth (D150ND0.5), (d) Double notch 1.0 mm depth (D150ND1.0), and (e) Double notch 2.5 mm depth (D150ND2.5)

The difference between both the simulation and experimental graphs produced with ABAQUS and the excitation of the impact hammer was shown. As stated by Dawari and Vesmawala [13], if the damage depth is too intact or deep in the structure then, the occurrence of damage to the structure will be increased. However, due to certain factors that were considered, the experimental data obtained was more unreliable. Therefore, the simulation results would be a guide, and the data obtained would be much more reliable compared to the experimental data.

4. Conclusions

A method for detecting damage in a beam was described in this study. In the CPR method, an FEA simulation and experimental FRF data were processed to determine the damage curvature as a function of frequency. The curvature was further processed using the cubic polynomial regression for curve fitting to obtain the undamaged data and damage index. The location of the damage, although inaccurate and imprecise, was revealed by spikes in the damage index.

Based on the comparisons of mode shape displacement between experimental and FEA, the average of the difference was less than 17% from nodes 12 until 15 for five specimens, and the overall difference was higher than that of the previously reported difference by Hasrizam and Fawazi [4], which was 3%. This inconsistency may have been due to the possible interference of noise, which cannot be ruled out, during the experimental modal test. In FEA simulation using ABAQUS, the CPR method indicated the presence of the damage index of two nearby small notches between Node 15 and Node 25, and Node 27 and Node 37 in single-notch specimens. In double-notch specimens, the CPR method indicated the presence of the damage index of four small notches between Node 10 to Node 17, Node 20 to Node 25, Node 27 to Node 33, and Node 35 to Node 43. Despite its inaccuracy and imprecision, the CPR method was still able to identify the damage for both the single and double-notch specimens, where the double-notch chart had multiple spikes in the damage index compared to the charts of the single-notch and control specimens. For experimental findings, it did not support the FEA results. These results could possibly have been due to the lack of an adequate filter for the CPR, which caused a deviation in the mode shape curvature between the damaged and undamaged structures, and the difference was implied as a false damage detection [4].

One advantage of this CPR method is that the procedure is simplistic, easy, and straightforward. However, when compared to the experimental modal test, this CPR method was unable to locate the precise location of the damage. Besides, this modal experimental test provided the CPR method, presented in this paper, with a much-impaired sensitivity when compared to the FEA simulation. An experimental demonstration of the method presented here showed that it can be significantly more susceptible to noise than some previously published procedures. The experiment was unsuccessful in locating notches due to several factors such as the elastic band, environment, humidity, and temperature.

There is room for further progress in determining the damage to the beam. The quantity of data or information gathered during the experimental testing was also due to the use of different types of calculation methods as comparisons. The calculation process was made easier through the use of a proper calculation software. In this research, the experimental data was taken from only 26 nodes for each specimen compared to the previous study, which used about 149 to 150 nodes. Since not enough

data was gathered for this research, therefore, the graph that was produced was not that smooth. In this research, only one curve fitting method, namely, a cubic polynomial regression, was implemented. At the same time, there are also other curve fitting techniques that can be used, such as the Robust Regression method studied by M H C Man et al.[14]. The method using Iteratively Re-weighted Least Square (IRLS) is able to reduce noise by minimizing the influence of an outlier towards estimation of undamaged Mode Shape Curvature.

Acknowledgement

The authors would like to express their appreciation to the Ministry of Higher Education of Malaysia (MOHE), Universiti Teknikal Malaysia Melaka (UTeM), and Universiti Teknologi Malaysia (UTM) for providing the facilities and funding to support the experimental and FEA simulation tasks. This work is supported by the Malaysian Government under the Fundamental Research Grant Scheme (FRGS/1/2018/TK03/UTM/02/12).

Nomenclatures

U_2 displacement mode shape

Greek Symbols

δ_i^m Damage index

$\omega_{d|i}$ Damaged mode shape curvature

$\omega_{u|CPR}$ Undamaged mode shape curvature Cubic Polynomial Regression

$\omega_{u|i}$ Undamaged mode shape curvature

Abbreviations

CF Chebyshev filters

CPR Cubic Polynomial Regression

FEA Finite Element Analysis

FRF Frequency Response Function

GSM Gapped Smoothing Method

ODE Ordinary Differential Equation

IRLS Iteratively Re-weighted Least Square

VBDD Vibration Based Damage Detection

References

1. Zou, Y.; Tong, I.; and Steven, G. (2020). Vibration-based model-dependent damage (delamination) identification and health monitoring for composite structures - A review. *Journal of Sound and Vibration*, 230(2), 357-378.
2. Woodford, C. (2018). Aluminum. Retrieved October 5, 2020, from <https://www.explainthatstuff.com/aluminum.html>.
3. Zhong, H.; and Yang, M. (2016). Damage detection for plate-like structures using generalized curvature mode shape method. *Journal of Civil Structure Health Monitoring*, 6(1), 141-152.

4. Hasrizam, C.M.; and Fawazi, N. (2017). Damage identification based on curvature mode shape using cubic polynomial regression and Chebyshev filters. In *IOP Conference Series: Materials Science and Engineering*, 271, 012091.
5. Yoon, M.K.; Heider, D.; Gillespie, J.; Ratcliffe, C.P.; and Crane, R.M. (2009) Local damage detection with the global fitting method using mode shape data in notched beams. *Journal of Nondestructive Evaluation*, 28, 63-74.
6. Rucevskis, S.; Sumbatyan, M.A.; Akishin, P.; and Chate, A. (2015). Tikhonov's regularization approach in mode shape curvature analysis applied to damage detection. *Mechanics Research Communications*, 65, 9-16.
7. Ratcliffe, C.P. (1997). Damage detection using a modified Laplacian operator on mode shape data. *Journal of Sound and Vibration*, 204(3), 505-517.
8. Abdel Wahab, M.M.; and De Roeck, G. (1999). Damage detection in bridges using modal curvatures: Application to a real damage scenario. *Journal of Sound and Vibration*, 226(2), 217-235.
9. Pandey, A.K.; Biswas, M.; and Samman, M.M. (1991). Damage Detection from changes in curvature mode shapes. *Journal of Sound and Vibration*, 145(2), 321-332.
10. Ratcliffe, C.P. (2000). A frequency and curvature based experimental method for locating damage in structures. *Journal of Vibration and Acoustics*, 122(3), 324-329.
11. Ratcliffe, C.P. and Bagaria, W.J. (1998). Vibration technique for locating delamination in a composite beam. *AIAA Journal*, 36(6), 1074-1077.
12. Hanly, S. (2018). 8 environmental factors affecting vibration measurement accuracy. Retrieved October 5, 2020, from <https://www.machinedesign.com/mechanical-motion-systems/press-release/21837096/8-environmental-factors-affecting-vibration-measurement-accuracy>.
13. Dawari, V.B.; and Vesmawala, G.R. (2013). Modal curvature and modal flexibility methods for honeycomb damage identification in reinforced concrete beams. *Procedia Engineering*, 51, 119-124.
14. Man, M.H.C.; Amiruddin, M.A.; and Fawazi, N. (2021). Evaluation of improved mode shape curvature-based damage detection using robust regression method. In *IOP Conference Series: Materials Science and Engineering*, 1092, 012036.